Eur J Nucl Med Mol Imaging (2014) 41:615–623
DOI 10.1007/s00259-013-2631-4

ORIGINAL ARTICLE

Image acquisition and interpretation criteria for ^{99m}Tc-HMPAO-labelled white blood cell scintigraphy: results of a multicentre study

Paola A. Erba · Andor W. J. M. Glaudemans · Niels C. Veltman · Martina Sollini · Marta Pacilio · Filippo Galli · Rudi A. J. O. Dierckx · Alberto Signore

Received: 31 July 2013 / Accepted: 6 November 2013 / Published online: 26 November 2013

Abstract
Purpose There is no consensus yet on the best protocol for planar image acquisition and interpretation of radiolabelled white blood cell (WBC) scintigraphy. This may account for differences in reported diagnostic accuracy amongst different centres.
Methods This was a multicentre retrospective study analysing 235 WBC scans divided into two groups. The first group of scans (105 patients) were acquired with a fixed-time acquisition protocol and the second group (130 patients) were acquired with a decay time-corrected acquisition protocol. Planar images were interpreted both qualitatively and semiquantitatively. Three blinded readers analysed the images.
Results The most accurate imaging acquisition protocol comprised image acquisition at 3 – 4 h and at 20 – 24 h in time mode with acquisition times corrected for isotope decay.
Conclusion Using this protocol, visual analysis had high sensitivity and specificity in the diagnosis of infection. Semiquantitative analysis could be used in doubtful cases, with no cut-off for the percentage increase in radiolabelled WBC over time, as a criterion to define a positive scan.

Keywords White blood cells · Scintigraphy · Infection imaging

Paola Erba and Andor Glaudemans contributed equally to this work.

P. A. Erba
Regional Center of Nuclear Medicine, Department of Translational Research and Advanced Technologies in Medicine, University of Pisa Medical School, Pisa, Italy

A. W. J. M. Glaudemans · R. A. J. O. Dierckx · A. Signore
Department of Nuclear Medicine and Molecular Imaging, University of Groningen, University Medical Center Groningen, Groningen, The Netherlands

N. C. Veltman
Department of Nuclear Medicine, Jeroen Bosch Hospital, 's-Hertogenbosch, The Netherlands

M. Sollini
Nuclear Medicine Unit, Department of Oncology and Advanced Technology, Arcispedale S. Maria Nuova – IRCCS, Reggio Emilia, Italy

M. Pacilio · F. Galli · A. Signore
Nuclear Medicine Unit, Department of Medical-Surgical Sciences and of Translational Medicine, Faculty of Medicine and Psychology, "Sapienza" University, Rome, Italy

A. Signore (✉)
Medicina Nucleare, Ospedale S. Andrea, University of Rome "Sapienza", Via di Grottarossa 1035, 00189 Roma, Italy
e-mail: alberto.signore@uniroma1.it

Introduction

The use of white blood cells (WBC) labelled with ^{99m}Tc-HMPAO or ^{111}In-oxine is still considered the gold standard nuclear imaging technique for the diagnosis of infections in the bone and soft tissue, except for spondylodiscitis [1, 2]. For acute osteomyelitis and for prosthetic joint infections, the reported diagnostic accuracy is approximately 90 % [3–5]. However, various studies have also shown lower rates for sensitivity and specificity. These differences in diagnostic accuracy reported for WBC scintigraphy may be related to different image acquisition protocols and different interpretation criteria [6, 7]. To strengthen the clinical use of WBC scintigraphy, procedures and protocols are being standardized throughout the world. To this end, the recently published

guidelines by the Infection Committee of the European Association of Nuclear Medicine (EANM) describe the indications, practical aspects, quality controls and safety procedures of this technique [8, 9]. Guidelines that describe the correct image acquisition and interpretation criteria for labelled WBC are also in preparation. Accurate acquisition protocols and interpretation criteria require knowledge of the normal biodistribution of radiolabelled WBC (i.e. blood and bone marrow) and pathological variants of WBC localization in different tissues and organs [2]. It is generally agreed that for osteomuscular infections and soft-tissue infections at least two imaging time-points are necessary, delayed (3 – 4 h after injection) and late (20 – 24 h). Early imaging (30 min to 1 h after injection), which may be a surrogate for bone marrow uptake, is optional. Image interpretation can be made qualitatively (visually) or semiquantitatively (by calculation). If the interpretation of planar images is doubtful and there is a suspicion of bone marrow expansion, bone marrow imaging with ^{99m}Tc-colloids is currently performed to reduce the false-positive rate [5, 10]. For exact localization of infection SPECT/CT may have added value [11].

In a large series of ^{99m}Tc-HMPAO-WBC planar scintigraph scans from patients with different types of infection, we retrospectively compared two different acquisition protocols (decay time-corrected, DTC, and fixed time, FT) and two different interpretation criteria (visual and semiquantitative evaluation), to determine the best combination for obtaining the highest diagnostic accuracy for infection versus sterile inflammation. The hypothesis was that a sterile inflammation will not show increased focal uptake with time, in contrast to an infection, and that this trend of an increase/decrease with time is more readily detectable using images acquired with a DTC acquisition than with a FT acquisition.

Materials and methods

Patient population

This was a retrospective study analysing data from patients referred for scintigraphy with ^{99m}Tc-HMPAO-labelled WBC from January 2009 to December 2011 in three university centres (University Medical Center Groningen, University of Pisa Medical School, and Sapienza University of Rome). Ethics committee of all the centres approved the study. We therefore analysed the data from 235 patients (115 from University Medical Center Groningen, 80 from University of Pisa Medical School, and 40 from Sapienza University of Rome) with suspected osteomyelitis, suspected prosthesis infection or suspected soft-tissue infection, as shown in Table 1. The patients included in Groningen were part of a larger series recently published [12]. Infection was suspected on the basis of clinical examination, blood tests (including WBC count, C-reactive protein, erythrocyte sedimentation rate, acute phase proteins), urine analysis, three sets of blood cultures including at least one aerobic and one anaerobic from a peripheral vein [13], and/or conventional radiology, e.g. plain radiography, ultrasonography and/or contrast-enhanced CT.

Table 1 Characteristics of the 235 patients

Characteristic	Value
Age (years)	
Mean	61
Median	63
Range	16-93
SD	17
Sex	
Female	131 (56 %)
Male	104 (44 %)
Type of suspected infection	
Osteomyelitis	80 (34 %)
Hip prosthesis	63 (27 %)
Knee prosthesis	66 (28 %)
Shoulder prosthesis	3 (1 %)
Soft tissue	23 (10 %)
Blood tests	
WBC counts	
Increased	13 (5 %)
Normal	134 (57 %)
C-reactive protein	
Increased	74 (31 %)
Normal	69 (29 %)
Erythrocyte sedimentation rate	
Increased	69 (29 %)
Normal	69 (29 %)

The final diagnosis of an infection or exclusion of an infection was defined on the basis of pathological, microbiological or clinical diagnosis, with clinical follow-up of more than 6 months in all patients. Overall, 109 patients were diagnosed with an infection and 126 were negative for infection (Table 2).

^{99m}Tc-HMPAO WBC preparation and imaging protocol

Preparation and labelling of WBC were performed according to the guidelines for the labelling of leucocytes with ^{99m}Tc-HMPAO of the European Association of Nuclear Medicine [8]. Radiolabelling efficiency was always in the range 70 – 85 %. In 105 patients, we used the FT acquisition protocol acquiring planar delayed and late images for 600 s each. In 130 patients, we used the DTC acquisition protocol acquiring planar (static) images at 0.5 – 1 h (optional "early images", 100 – 200 s), at 3 – 4 h ("delayed images",

Table 2 Final diagnosis in all patients and in the two groups studied with FT acquisition and DTC acquisition

Diagnosis	All patients, *n* (%)	FT acquisition, *n* (%)	DTC acquisition, *n* (%)
Infection			
Osteomyelitis	35 (32)	24 (69)	11 (31)
Infected hip prosthesis	23 (21)	8 (35)	15 (65)
Infected knee prosthesis	31 (28.4)	16 (52)	15 (48)
Infected shoulder prosthesis	3 (3)	3 (100)	0
Soft tissue infection	17 (15.6)	7 (41)	10 (59)
Total	109 (46.4)	58 (53)	51 (47)
No infection	126 (53.6)	48 (38)	78 (62)

133 – 300 s) and at 20 – 22 h ("late images", 951 – 2,396 s) after injection of 370 – 555 MBq ^{99m}Tc-HMPAO-labelled WBC (Table 3).

All images (128×128 matrix size or 256×256 matrix size , depending on centre) were acquired on a SPECT gamma camera system (Siemens Symbia T, Siemens Medical Systems, in Groningen; Hawkeye, GE Healthcare, in Pisa; SkyLight, Philips, in Rome) equipped with low-energy high-resolution collimators with the energy window centred at the 140 keV photopeak of ^{99m}Tc using a width of 20 %. All images were displayed and analysed using the same workstation (Osiris) to avoid differences in display of different camera systems. DTC images were displayed in number of counts using the same intensity scale both for delayed and late images, thereby avoiding operator bias in changing the intensity scale. This is essential when interpreting DTC images but it is not possible when images are acquired with a FT protocol. Therefore, FT images were displayed as percent of maximum counts as they usually appear in automatic mode on Siemens, GE and Philips workstations.

SPECT/CT was performed for precise location of infectious foci. In these patients, a low-dose CT transmission scan was acquired for 16 s over 220° for each transaxial slice. The full field of view consisting of 40 slices was completed in 10 min. The transmission data were reconstructed using filtered back-projection to produce cross-sectional images. The resolution of the CT scan was 2.2 mm and localization images were produced with a pixel size of 4.5 mm, similar to nuclear medicine emission images. The CT scans were reconstructed into a 256×256 matrix. The SPECT component of the same field of view was acquired using a 128×128 matrix, 360° rotation, 6° steps, and an acquisition of 40/60 s per frame at 4 and at 24 h, respectively. Both CT attenuation-corrected and noncorrected SPECT images were evaluated in the coronal, transaxial and sagittal planes, as well as in three-dimensional maximum intensity projection cine mode. Matching pairs of x-ray transmission and radionuclide emission images were fused using a Xeleris workstation (Pisa), and hybrid images of overlying transmission and emission data were generated.

Table 3 Examples of acquisition times for the DTC images acquired with ^{99m}Tc-HMPAO-WBC

	Time after the first acquisition (h)	Corrected acquisition time (s)	
		Early images acquired for 100 s	Early images acquired for 200 s
Delayed images	1.5	119	238
	2	126	252
	2.5	133	267
	3	141	283
	3.5	150	300
Late images	19.5	951	1902
	20	1007	2015
	20.5	1067	2135
	21	1131	2262
	21.5	1198	2396

Visual and semiquantitative image interpretation

The planar scintigraphic images were visually analysed separately by two experienced nuclear medicine physicians (P.E., A.G.); if the two observers disagreed, a third reader (A.S.) reviewed the images and his decision was considered as the final classification. The studies were classified as (a) "negative for infection" if no uptake was seen in both delayed and late planar images or when the uptake was the same or decreasing over time, and (b) "positive for infection" when at least one focus of abnormal uptake characterized by a time-dependent increase in radioactivity or an increase in size from the delayed to the late planar images was observed. In some positive patients with peripheral osteomyelitis, when differential diagnosis between bone and soft tissue involvement was not ascertained from planar images, we performed SPECT/CT for exact localization.

The visual analysis was performed using the same criteria for the images without decay correction and the DTC images. For semiquantitative analysis, in all images a region of interest (ROI) was drawn over the area of suspected infection and copied to presumed normal reference tissue (e.g. anterior superior iliac crest, unaffected contralateral bone, etc.) The

mean counts per pixel in these ROIs were recorded to calculate target/background (T/B) ratios in both delayed and late images. When the T/B ratios were similar or decreased with time the scan was considered negative for infection; when the T/B ratio increased with time, the scan was considered positive. Images were classified using different thresholds of increase in T/B ratio over time: ≤5, ≤10, ≤20 and ≤25 %.

Data analysis and statistics

The results of ^{99m}Tc-HMPAO-WBC scintigraphy were correlated with those of conventional radiological imaging and with the final microbiological, pathological or clinical diagnosis. For each patient the results of visual and semiquantitative interpretation were compared to the final diagnosis. Increases with time of <5 %, <10 %, <20 % and <25 %, were used in the semiquantitative analysis. All values are expressed as medians and range, as customary for nonparametric data. The two groups were compared in terms of clinical and demographic factors using Pearson's χ^2. The interobserver agreement rates were also evaluated and expressed as weighted kappa which corrects for agreement by chance. The sensitivity, specificity, diagnostic accuracy, negative predictive value (NPV) and positive predictive value (PPV) were calculated, and differences between groups compared using the chi-squared test. All statistical evaluations were performed using the STATA statistical software package, release 10-2010 (STATA Corporation, College Station, TX.).

Results

No significant differences in age distribution or any other clinical parameters between the two groups were observed. By adopting the interpretation criteria described above for scintigraphic detection of infection, it was possible to classify all the scans as either frankly positive or frankly negative; therefore there were no equivocal results. ^{99m}Tc-HMPAO-WBC scans were totally negative in 121 patients (47 of 105 FT acquisitions and 74 of 130 DTC acquisitions; p not significant). At least one abnormal area with focal accumulation of radiolabelled leucocytes with increases in radioactivity over time, or size, was detected in the remaining 114 patients (58 of 105 FT acquisition and 56 of 130 DTC acquisitions; p not significant). Table 4 shows the results of the visual analysis of the ^{99m}Tc-HMPAO-WBC scans in all patients and in relation to the specific clinical indication. Overall, DTC and FT acquisitions resulted in comparable sensitivity (94.1 % versus 94.8 %; p not significant) and NPV (96.3 % versus 93.3 %; p not significant), but DTC resulted in better specificity (100 % versus 89.4 %; $p=0.006$), accuracy (97.7 % versus 92.4 %; $p=0.05$) and PPV (100 % versus 91.6 %; $p=0.05$). Figure 1 shows examples of radiolabelled WBC scans positive and negative by visual analysis. Even though the numbers of patients with the specific clinical indications varied, the performance of DTC acquisition in the visual analysis was consistently better, except in the diagnosis of soft-tissue infections (Table 4).

In the semiquantitative analysis the best accuracy, sensitivity and NPV were found considering any percentage increase in radioactivity in the suspected lesion over time with both the FT and DTC acquisitions. In contrast, the specificity and PPV increased with increasing percentage increase threshold (Table 5). Furthermore, accuracy, specificity and PPV were generally higher in the semiquantitative analysis when the images were acquired with the FT acquisition, whereas sensitivity and NPV were higher when the images were acquired with the DTC acquisition (Table 6). This was particularly true for osteomyelitis and hip prosthesis, but not for soft-tissue infections or knee prosthesis. Figure 2 provides examples of visual and semiquantitative interpretation of images.

Interobserver agreement rates for the interpretation of ^{99m}Tc-HMPAO-WBC images were higher for DTC images as compared to FT images (lack of consensus in 11 % and 19 % of scans, respectively, with the lower agreement for hip and knee prosthesis infections). The rate of concordance

Table 4 Diagnostic performance of qualitative (visual) analysis of ^{99m}Tc-HMPAO-WBC scintigraphy images in relation to the final diagnosis

	Osteomyelitis		Hip prosthesis		Knee prosthesis		Soft tissue		Total	
	FT	DTC	FT	DTC	FT	DTC	FT	DTC	FT	DTC
True positive (n)	23	11	7	14	15	14	7	9	55[a]	48
True negative (n)	23	20	10	29	8	25	1	5	42	79
False positive (n)	2	0	1	0	2	0	0	0	5	0
False negative (n)	1	0	1	1	1	1	0	1	3	3
Sensitivity (%)	96	100	87	93	94	93	100	90	95	94
Specificity (%)	92	100	91	100	80	100*	100	100	89	100*
Accuracy (%)	94	100	89	98	88	98*	100	93	92	98*
PPV (%)	92	100	87	100	88	100*	100	100	92	100*
NPV (%)	96	100	90	93	89	93	100	83	93	96

*$p<0.05$ versus FT

[a] Includes three patients with a shoulder prosthesis

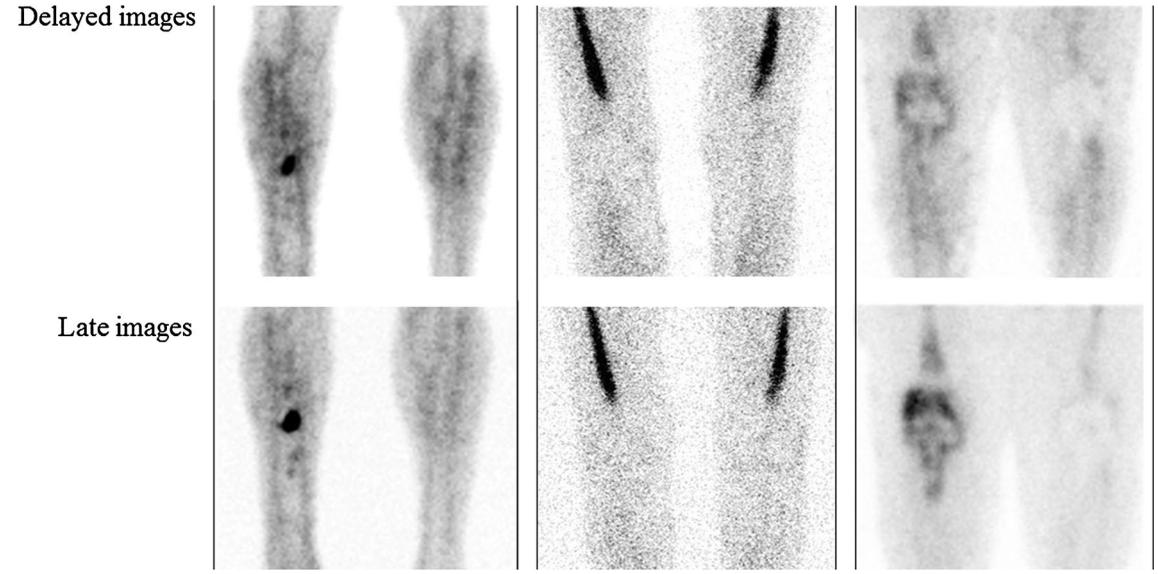

Fig. 1 ^{99m}Tc-HMPAO-WBC scintigraphy images in patients with suspected bone and knee prosthesis infections. The images were acquired after 4 h (delayed images) and 20 h (late images) with either FT acquisition (*left* and *centre*) or DTC acquisition (*right*). In all cases visual analysis correctly diagnosed osteomyelitis (*left*), aseptic bone marrow expansion (*centre*) and infected prosthesis (*right*) in the right knee versus the left knee

between the visual and the semiquantitative analyses was better for any percent increase in radioactivity over time and for the DTC images (200 of 235) either considering all patients together or considering those with osteomyelitis and prosthetic infections separately. In patients with soft-tissue infection, the best agreement was obtained comparing the visual and the semiquantitative analysis considering a 5 % of increase in radioactivity over time (always better for the DTC images).

Discussion

It is commonly accepted that WBC images are visually classified as (1) negative if no uptake or a decrease in uptake from delayed to late images is present, (2) positive when uptake is seen in both delayed and late images with an increase in activity or size over time, and (3) equivocal when uptake in delayed and late images is the same or slightly decreased. However, general criticisms of the visual analysis are that it is strictly operator-dependent and that the final results may differ significantly between acquisition and display using different contrasts and backgrounds. Acquisition protocols are variable. In some protocols, early, delayed and late images may be acquired with a fixed constant time for all images, and in others all images may be acquired with a fixed number of counts, but both methods are not corrected for isotope decay, are influenced by variations in background activity and are operator-dependent. To reduce variability some authors suggest that, after acquisition, images are displayed equalizing

Table 5 Diagnostic performance of semiquantitative analysis of ^{99m}Tc-HMPAO-WBC scintigraphy images in relation to the final diagnosis for both acquisition protocols

	Any T/B ratio increase		T/B ratio increase >5 %		T/B ratio increase >10 %		T/B ratio increase >20 %		T/B ratio increase >25 %	
	FT	DTC	FT	DTC	FT	DTC	FT	DTC	FT	DTC
True positive (*n*)	56	48	46	38	41	34	30	24	26	18
True negative (*n*)	34	59	40	65	45	69	45	69	45	69
False positive (*n*)	13	20	6	15	2	10	2	10	2	10
False negative (*n*)	2	3	13	12	17	17	28	27	32	33
Sensitivity (%)	97	94	78	76	71	67	52	47	45	35
Specificity (%)	72	75	87	81	96	87	96	87	93	87
Accuracy (%)	86	82	82	79	82	79	71	72	68	67
PPV (%)	81	70	87	72*	95	77*	94	71*	96	64*
NPV (%)	94	95	75	84	73	80	62	72	58	68

*$p < 0.05$ versus FT

Table 6 Diagnostic performance of semiquantitative analysis of ^{99m}Tc-HMPAO-WBC scintigraphy images in relation to the specific indications and compared with the final diagnosis for both acquisition protocols

	Osteomyelitis		Hip prosthesis		Knee prosthesis		Soft tissue	
	FT	DTC	FT	DTC	FT	DTC	FT	DTC
True positive (*n*)	23	11	7	14	16	14	7	9
True negative (*n*)	23	17	9	20	6	17	1	5
False positive (*n*)	2	3	2	9	4	8	0	0
False negative (*n*)	1	0	1	1	0	1	0	1
Sensitivity (%)	96	100	88	93	100	93	100	90
Specificity (%)	92	85	82	69	60	68	100	100
Accuracy (%)	94	90	84	77	85	78	100	93
PPV (%)	92	79	78	61	80	64*	100	100
NPV (%)	96	100	90	95	100	94	100	83

*$p < 0.05$ versus FT

bone marrow activity as reference. However, bone marrow activity may also change over time, and therefore this modality for displaying images does not improve accuracy and is limited to expert readers and some regions of the body with good bone marrow activity.

We suggest that images are acquired at different time-points with different acquisition times, starting from a settled amount of time in the early images and deriving the corresponding acquisition times for delayed and late images by correction for isotope decay (as shown in Table 3). As a result, delayed and late images have the same count statistics as early images, and comparison is possible, reducing operator bias [14–16]. It is of course mandatory to display all images with the same intensity scale in count units and not in percentage of maximum counts per pixel, another common display error. If images are correctly acquired and displayed, they are operator-independent, reproducible, comparable and easy to interpret. We used the same software system (Osirix) in all patients in order to avoid differences in display of different software systems between the centres. However, all data were reproducible on all three systems (GE, Philips and Siemens) by displaying images in count units with the same intensity scale.

Semiquantitative analysis may also be helpful when visual interpretation is doubtful. ROIs can be drawn over the part of the presumed infected focus, copied to presumed normal reference tissue (e.g. anterior superior iliac crest, contralateral bone), and T/B ratios calculated. However, the location of ROIs in a lesion and reference tissue is operator-dependent. Additionally, the level of significance of the T/B ratios is

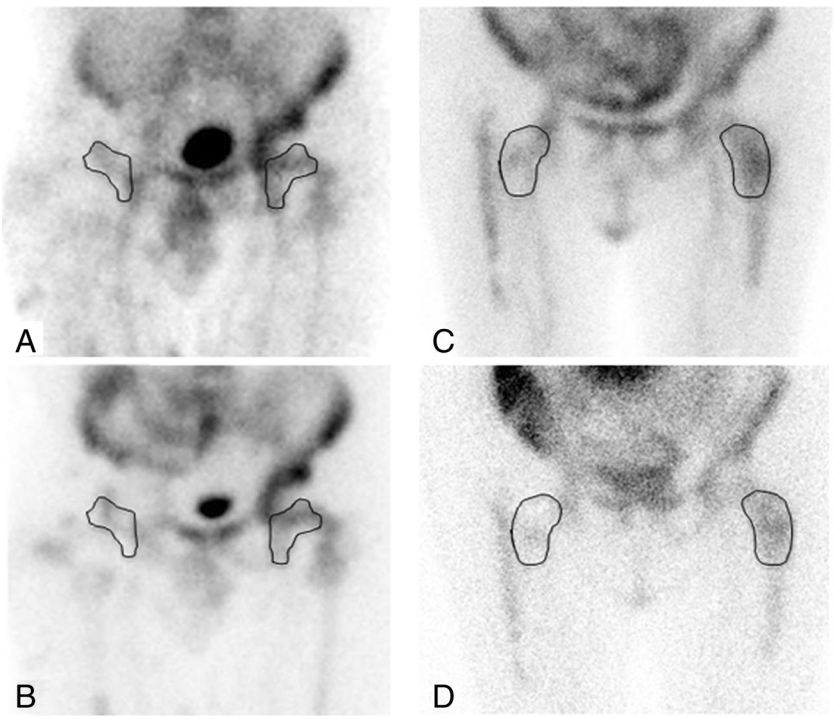

Fig. 2 ^{99m}Tc-HMPAO-WBC scintigraphy images in two patients with suspected low-grade infection of a right hip prosthesis. The images were acquired after 4 h (*top*) and 20 h (*bottom*) using FT acquisition (*left*) or DTC acquisition (*right*). **a**, **b** Visual analysis was negative and semiquantitative analysis showed a stable T/B ratio over time (equivocal for infection). After prosthesis removal, microbiology showed the presence of infection. **c d** Visual analysis was negative and semiquantitative analysis showed a stable T/B ratio over time (equivocal for infection). After prosthesis removal, microbiology confirmed the absence of infection. These two examples highlight how DTC acquisition allows accurate and easier visual interpretation of images

arbitrarily decided, and no studies have yet defined the threshold increase in radiolabelled WBC over time that should be considered positive.

In this study, we retrospectively compared two different acquisition protocols for planar images (DTC and FT) and two different interpretation approaches (visual and semiquantitative) to determine the criteria allowing the highest diagnostic performances. The best results were obtained with DTC images and visual analysis for bone-associated infections but not for soft-tissue infections. Despite the fact that statistical significance was reached only when considering the whole group of patients, for each bone indication a consistent improvement in the diagnostic performances was always achieved by acquiring DTC images. The added value of DTC acquisition was more evident in patients with bone and prosthetic infections, and thus the use of DTC acquisition potentially limits the need for bone marrow imaging with colloids. The FT images possibly had an advantage in term of sensitivity, but FT acquisition resulted in a significant decrease in specificity and diagnostic accuracy. On the other hand, when soft-tissue infections were considered, the advantage of DTC acquisition was not evident. This may have several explanations. First, there might be different kinetics of migration of radiolabelled WBC in bone and soft tissue. Additionally, soft-tissue infections include muscle, brain, abdomen, heart, lung and skin infections, are thus a very heterogeneous group with possible different behaviours in terms of leucocyte recruitment, and may need "ad hoc" interpretation criteria as already demonstrated for dermal filler infections and dermal infections in diabetic foot [14, 15]. In our study the seven patients with soft-tissue infections imaged with FT acquisition mainly had muscle infections, whereas the ten patients with soft-tissue infections imaged with DTC acquisition all had skin infections, and this difference may account for the different accuracies in the results.

Overall, the main advantage of a DTC acquisition protocol is represented by the absence of operator interference and bias that, by contrast, can strongly affect the results with FT acquisition. Indeed, DTC images were displayed in number of counts, using the same intensity scale both for delayed and late images, thereby avoiding operator bias introduced by changing the intensity scale. This is essential when interpreting

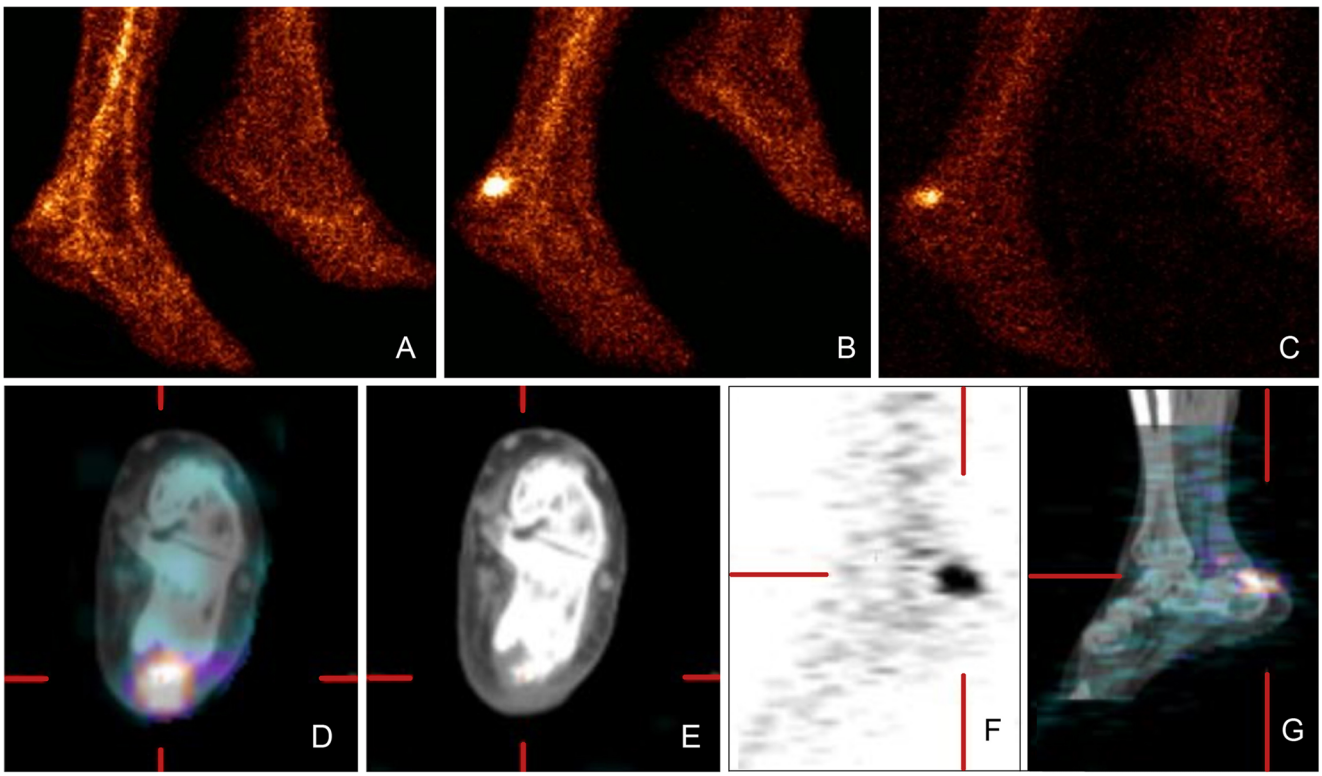

Fig. 3 Planar images of the feet of a patient with a suspected osteomyelitis consequent upon fracture of the calcaneus bone with a cutaneous wound. **a** At 30 min after injection the "early image" was acquired for 100 s per frame (61,269 counts). **b** At 3 h after injection (2.5 h after the first image) the "delayed image" was acquired for 133 s per frame (52,274 counts). **c** At 20 h after injection (19.5 h after the first image) the "late image" was acquired for 951 s per frame (52,212 counts) and clearly shows a decrease in activity on visual analysis, a sign of no osteomyelitis. Semiquantitative analysis showed T/B ratios of 2.2 at 3 h and 1.8 at 20 h, confirming a decrease with time, a sign of no infection, just wound inflammation. **d**–**g** SPECT/CT images at 20 h, however, do not allow the origin of the uptake (cutaneous versus bone surface) to be clearly identified, and thus the visual analysis of planar images is more accurate. The patient was operated upon to remove the bone fragment, and no sign of osteomyelitis was confirmed on histology

DTC images but it is not possible when images are acquired with a FT protocol. In this study there was little difference, although significant, in global diagnostic accuracy between the FT and DTC acquisitions (92.4 % versus 97.7 %; $p < 0.05$), but it is worth bearing in mind that the readers were also experts in reading FT images. Indeed, we can expect that readers with less expertise will achieve a lower diagnostic accuracy in reading FT images, thus making DTC acquisition even more relevant.

Our results indicate that any percentage increase in radioactivity over time leads to high sensitivity (Table 5). Increasing the threshold to, for example, 20 % radioactivity increase over time improves specificity, but lowers sensitivity. The threshold for percentage T/B ratio increase over time may be affected by several parameters such as the type of infection (acute versus chronic), the type of infection (osteomyelitis versus soft tissue), the sustaining microorganisms and the presence of concomitant antimicrobial treatment. Since all these factors can significantly modify the intensity and pattern of radiolabelled WBC over time, further studies are warranted to obtain clinical validation of this approach.

Another point of discussion is the placement of the ROIs, which can differ between operators (contralateral, bone marrow, etc.). Although a recent study by our group has shown that the contralateral region is the most accurate for positioning the ROI for the background semiquantitative calculation [17], in this study it was not possible to apply this approach, and background ROIs were positioned either on ipsilateral bone marrow or muscle when contralateral bone marrow was not available.

To better localize the site and extent of infection, SPECT/CT images may be used. If sequential SPECT images are acquired, acquisition times for SPECT can also be normalized according to isotope decay using the same decay formula as shown in Table 3. SPECT/CT is invaluable to better identify the site and delineate the extent of ^{99m}Tc-HMPAO-WBC uptake (i.e. bone or soft tissue) as compared to planar and stand-alone SPECT images due to the easy identification of blood-pool activity either in the vascular bed or bone marrow or, for example, nonspecific accumulation of ^{99m}Tc-HMPAO in the bowel. In this study, however, SPECT/CT was not used for diagnosing infection but for determining its extent in positive planar images. The role of SPECT/CT has been established for the detection of soft-tissue infections [15] and endocarditis, cardiac devices, vascular prosthesis infections [11] and diabetic foot [18] when anatomical landmarks are needed. However, in some circumstances intense uptake of the radiolabelled WBC localized close to bone may lead to false-positive results for osteomyelitis (see Fig. 3).

When evaluating bone/prosthesis infections and soft-tissue infections, whole-body imaging is mostly not necessary. However, such images allow a normal biodistribution of the radiolabelled autologous leucocytes to be checked and also allow the detection of distant sites of infection when suspected. In sequential whole-body imaging, acquisition times can also be normalized.

Finally, to refute the general perception that DTC acquisition protocols are time-consuming procedures, particularly for acquisition of late images, in the majority of the patients early images can be acquired for 100 or 200 s (depending on whether the injected activity is above 20 mCi or between 10 and 20 mCi), with acquisition times for late images of about 1,000 or 2,000 s that is usually well tolerated by the majority of the patients.

Conclusion

In a patient with suspicion of a prosthetic joint infection or osteomyelitis, WBC scintigraphy should be performed acquiring images at least at two time-points, at 3 – 4 h (delayed images) and at 20 – 24 h (late images). Early images (at 0.5 – 1 h after injection) may also be acquired to provide an early map of bone marrow distribution, but are not strictly necessary. The most reproducible and accurate acquisition protocol in musculoskeletal infections is a DTC acquisition. Images must then be displayed using the same intensity scale in count units and not as percentage of maximum counts per pixel. When these methodological considerations are fulfilled, visual analysis of images is operator-independent and is enough for high diagnostic accuracy of infection, thus avoiding semiquantitative analysis.

Conflicts of interest None.

References

1. Van der Bruggen W, Bleeker-Rovers CP, Boerman OC, Gotthardt M, Oyen WJ. PET and SPECT in osteomyelitis and prosthetic bone and joint infections: a systematic review. Semin Nucl Med. 2010;40:3–15.
2. Signore A, Glaudemans AW. The molecular imaging approach to image infections and inflammation by nuclear medicine techniques. Ann Nucl Med. 2011;25:681–700.
3. Palestro CJ, Love C, Bhargava KK. Labeled leukocyte imaging: current status and future directions. Q J Nucl Med Mol Imaging. 2009;53:105–23.
4. Love C, Marwin SE, Palestro CJ. Nuclear medicine and the infected joint replacement. Semin Nucl Med. 2009;39:66–78.
5. Gemmel F, Van den Wyngaert H, Love C, Welling MM, Gemmel P, Palestro CJ. Prosthetic joint infections: radionuclide state-of-the-art imaging. Eur J Nucl Med Mol Imaging. 2012;39:892–909.
6. Tondeur MC, Sand A, Ham HH. Interobserver reproducibility in the interpretation of 99mTc-labelled white blood cell scintigraphic images. Nucl Med Commun. 2008;29:1093–9.
7. Glaudemans AW, Galli F, Pacilio M, Signore A. Leukocyte and bacteria imaging in prosthetic joint infections. Eur Cell Mater. 2013;25:61–77.

8. De Vries EF, Roca M, Jamar F, Israel O, Signore A. Guidelines for the labelling of leucocytes with (99m)Tc-HMPAO. Inflammation/infection Taskgroup of the European Association of Nuclear Medicine. Eur J Nucl Med Mol Imaging. 2010;37:842–8.
9. Roca M, De Vries EF, Jamar F, Israel O, Signore A. Guidelines for the labelling of leucocytes with (111)In-oxine. Inflammation/infection Taskgroup of the European Association of Nuclear Medicine. Eur J Nucl Med Mol Imaging. 2010;37:835–41.
10. Gotthardt M, Bleeker-Rovers CP, Boerman OC, Oyen WJ. Imaging of inflammation by PET, conventional scintigraphy, and other imaging techniques. J Nucl Med. 2010;51:1937–49.
11. Erba PA, Conti U, Lazzeri E, Sollini M, Doria R, De Tommasi SM, et al. Added value of 99mTc-HMPAO labeled leukocyte SPECT/CT in the characterization and management of patients with infectious endocarditis. J Nucl Med. 2012;53:1235–43.
12. Glaudemans AWJM, de Vries EFJ, Vermeulen LEM, Slart RHJA, Dierckx RAJO, Signore A. A large retrospective single-centre study to define the best image acquisition protocols and interpretation criteria for white blood cell scintigraphy with 99mTc-HMPAO-labelled leukocytes in musculoskeletal infections. Eur J Nucl Med Mol Imaging. 2013;40:1760–9.
13. Raoult D, Casalta JP, Richet H, et al. Contribution of systematic serological testing in diagnosis of infective endocarditis. J Clin Microbiol. 2005;43:5238–42.
14. Familiari D, Glaudemans AW, Vitale V, Prosperi D, Bagni O, Lenza A, et al. Can sequential 18F-FDG PET/CT replace WBC imaging in the diabetic foot? J Nucl Med. 2011;52:1012–9.
15. Grippaudo FR, Pacilio M, Di Girolamo M, Dierckx RA, Signore A. Radiolabelled white blood cells in the work out of dermal filler complications. Eur J Nucl Med Mol Imaging. 2013;40:418–25.
16. Signore A. Techniques, image acquisition and interpretation criteria. In: Signore A, Quintero AM, editors. Diagnostic imaging of infections and inflammatory diseases: a multidisciplinary approach. New York: Wiley; 2013. p. 149–67.
17. Glaudemans AW, De Vries EF, Vermeulen LE, Slart RH, Dierckx RA, Signore A. A large retrospective single-centre study to define the best image acquisition protocols and interpretation criteria for white blood cell scintigraphy with 99mTc-HMPAO-labelled leucocytes in musculoskeletal infections. Eur J Nucl Med Mol Imaging. 2013;40:1760–9.
18. Schillaci O. Hybrid imaging systems in the diagnosis of osteomyelitis and prosthetic joint infection. Q J Nucl Med Mol Imaging. 2009;53:95–104.